Front. Phys. 10, 104201 (2015)
DOI 10.1007/s11467-014-0452-y

RESEARCH ARTICLE

Transmission, reflection, scattering, and trapping of traveling discrete solitons by $\mathcal{C}$ and $\mathcal{V}$ point defects

Jin-Hong Huang[1], **Hong-Ji Li**[1], **Xiang-Yu Zhang**[1,2], **Yong-Yao Li**[1,†]

[1] *Department of Applied Physics, South China Agricultural University, Guangzhou 510642, China*
[2] *Department of Electrical and Computer Engineering, Duke University, Durham, NC 27708, USA*
Corresponding author. E-mail: †*yongyaoli@gmail.com*
Received May 16, 2014; accepted July 24, 2014

We study the interactions of moving discrete solitons in waveguide arrays with two types of point defects that are constructed by varying either the local linear coupling or local waveguide propagation constant at the center of the waveguide array. A broad discrete soliton is kicked toward the defect and interacts with it. Transmission, reflection, scattering, and trapping during the interaction between the soliton and the defect occur depending on the parameters. The detailed behavior of the soliton dynamics is analyzed numerically. A transmission window in the parameter domain is found and the behavior of this window for different parameters is studied. The dynamics of the soliton in the transmission window is found to have chaotic features under certain circumstances and the causes of these phenomena are identified and discussed.

Keywords traveling discrete soliton, waveguide arrays, $\mathcal{C}$-defect and $\mathcal{V}$-defect

PACS numbers 42.65.Tg, 42.65.Wi, 42.82.Et

1 Introduction

Optical fields propagating in discrete periodic systems provide many functionalities that are impossible to achieve in the bulk. Arrays of evanescently coupled waveguides made of nonlinear materials are the fundamental model of discrete optics [1–5]. The paraxial propagation of a light field in the waveguide arrays can be described by the discrete nonlinear Schrödinger equation. Many exciting phenomena including discrete and anomalous diffraction, negative refraction, and Bloch oscillation of light in both one-dimensional (1D) and two-dimensional (2D) systems, have been experimentally demonstrated. Among these phenomena, much attention has been given to self-trapping of light in nonlinear optical waveguide arrays or lattices, namely, discrete solitons. Discrete solitons' energy resides primarily in distinct waveguide sites and exists through a balance of discrete diffraction effects and nonlinearity. Unlike their continuous counterparts, discrete solitons represent collective excitations of a nonlinear chain (array); consequently, it was predicted that discrete solitons in nonlinear waveguide array networks can provide a rich environment for all-optical data processing applications. They can realize intelligent functional operations such as routing, blocking, logic functions and time-gating [6]; thus, discrete waveguide arrays have the potential to become an important device in all-optical switching networks, like semiconductor devices in electronic circuits. Therefore, the formation and control of discrete solitons in different functional systems has become a hot topic in optical science and its applications.

An essential topic for the application of discrete solitons is control of their motion along waveguide arrays. Many papers have discussed how to move a discrete soliton in a lattice (or waveguide array) while maintaining its shape (i.e., not exciting phonon modes in any conspicuous form) [7–9]. However, there is still no clear conclusion. Generally, discrete soliton solutions with zero transverse velocity can be subdivided into two basic categories: (i) those at the base of the band (fundamental discrete solitons in a self-focusing nonlinearity) and (ii) those at the edge of the band (staggered solitons in a self-defocusing nonlinearity). These solitons are strongly pinned, if their width is narrow. However, if a discrete soliton is broad enough, it becomes a quasi-continuous object that shows obvious mobility, and can be partially explained by the Ablowitz–Ladik model [10–12].

The other essential topic is the design of a functional waveguide array system. It is well known that defects significantly enhance the functionality of a periodic system.

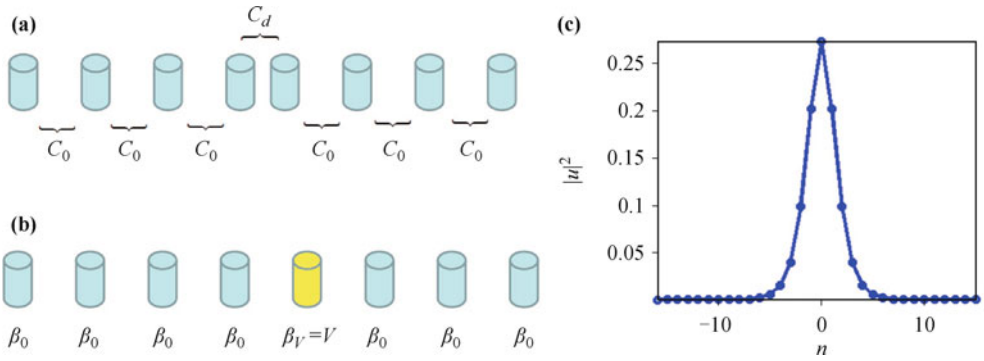

Fig. 1 **(a)** 1D waveguide array is embedded by a $\mathcal{C}$ point defect, where the coupling parameter at the defect (between the two centered waveguides) is different from others. **(b)** 1D waveguide array is embedded by a $\mathcal{V}$ point defect, where the propagation constant of the defect waveguide (the yellow color waveguide) is different from others. **(c)** A typical example of stable broad discrete soliton with $P = 1$, $C_d = C_0 \equiv 0.5$, $\beta_n \equiv 0$ and $\gamma = -1$ (note that this soliton is produced from a normal waveguide array without any defect).

For example, semiconductor crystals that exhibit defects can lead to both bulk and surface electronic states that ultimately affect charge transport processes. Hence, the topic of light wave propagation in waveguide arrays with embedded defects also motivates many studies [13–23].

In this work, we study the interaction of moving 1D discrete solitons with two types of local point defects, denoted by $\mathcal{C}$ and $\mathcal{V}$. These two types of point defects are embedded into the waveguide arrays [see Figs. 1(a) and (b)]. The effects of the defects on the moving solitons are identified using numerical simulations. The model is described in Section 2 of this paper, and the numerical results and related discussion are presented in Section 3. This work is concluded in Section 4.

2 The model

The models used in this work are displayed schematically in Figs. 1(a) and (b). A 1D waveguide array has two types of point defects embedded in the center of the array. In the first type, the coupling parameter where the defect is located differs from the others, and in the second type, the propagation constant of the waveguide where the defect is located differs from that of the other waveguides. These two types of defect are well established in experiments; the former can be produced by tuning the distance between two adjacent waveguides at the location of the defect, and the latter can be produced by doping impurities to change the refractive index of the defect waveguide. The propagation of the light field along these two types of waveguide arrays can be described by

$$\mathrm{i}\frac{\mathrm{d}u_n}{\mathrm{d}z} = -\left(C_{n-1,n}u_{n-1} + C_{n,n+1}u_{n+1}\right) + \beta_n u_n + \gamma|u_n|^2 u_n, \tag{1}$$

where u_n is the amplitude of light at waveguide n, z is the propagation distance, $C_{n,n+1}$ is the coupling parameter between waveguides n and $n+1$, β_n is the propagation constant of waveguide n, and γ is the nonlinear parameter of the waveguide array. Here, we fix $\gamma = -1$, at which value the waveguide array features a self-focusing nonlinearity.

For the model in Fig. 1(a), the parameters of the waveguide arrays are set to

$$C_{n,n+1} = \begin{cases} C_\mathrm{d}, & n = N/2 \\ C_0, & n \neq N/2, \end{cases} \qquad \beta_n \equiv \beta_0, \tag{2}$$

where C_0 and β_0 are constants. Because defects of this type are governed by the coupling parameters, we call them $\mathcal{C}$ defects. For the model in Fig. 1(b), the parameters are set to

$$C_{n,n+1} \equiv C_0, \tag{3}$$

$$\beta_n = \begin{cases} V, & n = N/2+1, \\ \beta_0, & n \neq N/2+1. \end{cases}$$

Because β_n in Eq. (1) acts as the effective potential, we call defects of this type as $\mathcal{V}$ defects. Eqs. (3) and (4) describe those two defects, respectively, embedded in the center of the waveguide array. The objective of this work is to study the interactions between a moving discrete soliton and these two types of point defect. Our studies are conducted in the following sequence. (i) First, we build a stationary broad discrete soliton, U_n, which is produced by a normal defect-free waveguide array. The total power of this soliton is defined as

$$P = \sum_n |u_n|^2. \tag{4}$$

A typical example of such a soliton is shown in Fig. 1(c). As discussed above, a moving soliton in this system should be broad, so it becomes a quasi-continuous

object; therefore, its total power cannot be too large because otherwise it will become narrow, be pinned onto the lattice, and become immobile. Thus, the waveguide system has a threshold power above which the discrete soliton stops moving [10]; for our system, this power is 2. Second, we place the soliton solution into the waveguide array at a distance n_0 from the defect; then, we construct a traveling soliton by applying a kick to it. This operation is expressed as

$$u(P,\eta,n_0,z=0)=U_{n-n_0}(P)\mathrm{e}^{\mathrm{i}\eta(n-n_0)}, \tag{5}$$

where η is the strength of the kick applied to the soliton solution U_{n-n_0}. Third, we study the dynamical process by which the traveling soliton interacts with the defects by direct simulation of Eq. (1) with the initial condition (5).

3 Results and discussion

Eq. (1) is directly simulated using the four-step Runge–Kutta method. The stationary soliton solutions are produced by the imaginary time propagation method [24, 25]. In the numerical simulations, we set the total number of waveguide sites to $N=128$ ($n\in[-64,63]$), and fix $n_0=-32$. For convenience, we fix $C_0=0.5$ and $\beta_0=0$, and leave (P,η,C_d,V) as a controllable parameter.

Figures 2 and 3 show typical examples of the behavior of traveling solitons interacting with $\mathcal{C}$ and $\mathcal{V}$ defects. We found that transmission, reflection, scattering, and trapping of the solitons can be found in both cases. To identify the causes of these behaviors, we define the transmissivity and reflectivity for the $\mathcal{C}$ and $\mathcal{V}$ defect, respectively, as

$\mathcal{C}$ defect:

$$T=\frac{\sum_{n=N/2+1}^{N}|u_n|^2}{P}\times 100\%,$$
$$R=\frac{\sum_{n=1}^{N/2}|u_n|^2}{P}\times 100\%, \tag{6}$$

$\mathcal{V}$ defect:

$$T=\frac{\sum_{n=N/2+2}^{N}|u_n|^2+|u_{N/2+1}|^2/2}{P}\times 100\%,$$
$$R=\frac{\sum_{n=1}^{N/2}|u_n|^2+|u_{N/2+1}|^2/2}{P}\times 100\%. \tag{7}$$

Figures 4(a) and (b) display T and R versus C_d (the strength of the $\mathcal{C}$ defect) and V (the strength of the $\mathcal{V}$ defect), respectively. A general pattern can be inferred from these figures. In the absence of defects, i.e., $C_d/C_0=1$ and $|V|=0$, $T=100\%$ and $R=0\%$, which is expected because there is no defect. When the strength

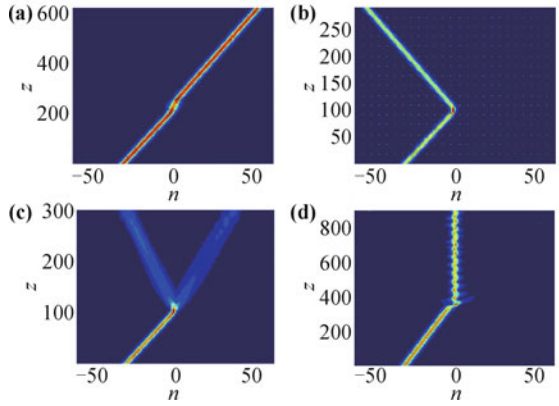

Fig. 2 Typical examples of behaviors of traveling soliton interact with $\mathcal{C}$ defect. **(a)** Transmission $[(P,\eta,C_d)=(1,\pi/20,0.96)]$; **(b)** Reflection $[(P,\eta,C_d)=(1,\pi/9,0.6)]$; **(c)** Scattering $[(P,\eta,C_d)=(1,\pi/9,0.82)]$; **(d)** Trapping $[(P,\eta,C_d)=(1,\pi/36,1.12)]$.

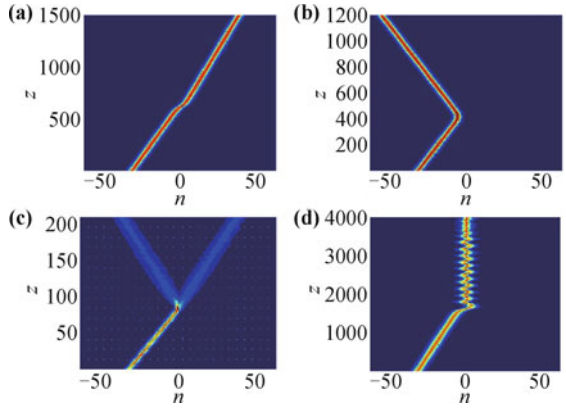

Fig. 3 Typical examples of behaviors of traveling soliton interact with $\mathcal{V}$ defect. **(a)** Transmission $[(P,\eta,V)=(1,\pi/60,-0.02)]$; **(b)** Reflection $[(P,\eta,V)=(1,\pi/45,-0.86)]$; **(c)** Scattering $[(P,\eta,V)=(1,5\pi/35,0.28)]$; **(d)** Trapping $[(P,\eta,V)=(0.8,\pi/180,-0.02)]$.

of the defect increases, i.e., C_d/C_0 deviates from 1 and $|V|$ deviates from 0, T decreases and R increases, which means that some of the energy of the soliton is transmitted across the defect, and some is reflected by the defect; thus, the soliton is destroyed in this case. When the strength of the defect is strong enough, i.e., $C_d/C_0\to 0$ or $\gg 1$ and $|V|\gg 0$, then $T\to 0\%$ and $R\to 100\%$, and the traveling soliton is totally reflected by the defect. Between the areas of total transmittion and total reflection, there are two special points, which are the intersections of the T and R curves. At these points, $T=R=50\%$, which means that the soliton is divided into two equal segments by the defect and is totally destroyed. Typical examples of soliton scattering at these points are shown in Figs. 2(c) and 3(c) for the $\mathcal{C}$ and $\mathcal{V}$ defect, respectively. We called them the left scattering point (LSP, on the left side) and right scattering point (RSP, on the right side) [see Fig. 5(a)]. Figure 5 shows the LSP and RSP as func-

tions of P and η for $\mathcal{C}$ and $\mathcal{V}$ defects. In Fig. 4, we can see that in the parameter domain between the LSP and RSP, traveling solitons feature mainly transmission, which occurs within a transmission window, whereas outside of this window, the solitons feature mainly reflection. Figure 5 shows that this transmission window becomes narrower as η decreases and P increases. This phenomenon is well understood, because the value of η dominates the

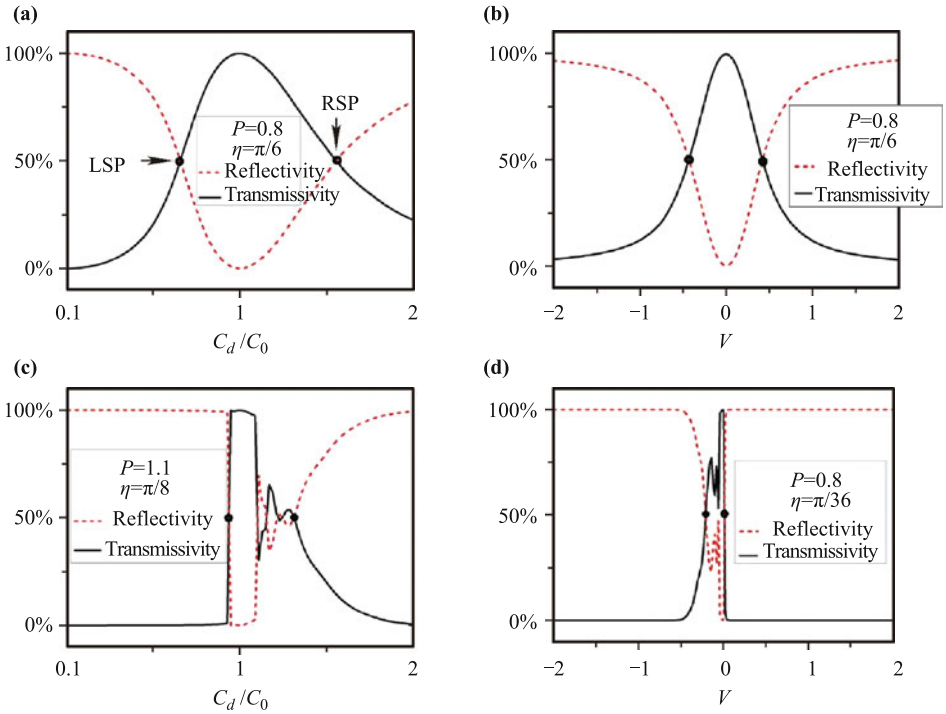

Fig. 4 Typical examples of the curves of transmissivity and reflectivity as function of C_d and V. The black solid curves and the red dash curves are transmissivity and reflectivity, respectively. The two black spots represent the LSP (left side) and RSP (right side), respectively. **(a)** T and R vs. C_d/C_0 with $(P, \eta) = (0.8, \pi/6)$, **(b)** T and R vs. V with $(P, \eta) = (0.8, \pi/6)$, **(c)** T and R vs. C_d/C_0 with $(P, \eta) = (1.1, \pi/18)$, **(d)** T and R vs. V with $(P, \eta) = (0.8, \pi/36)$.

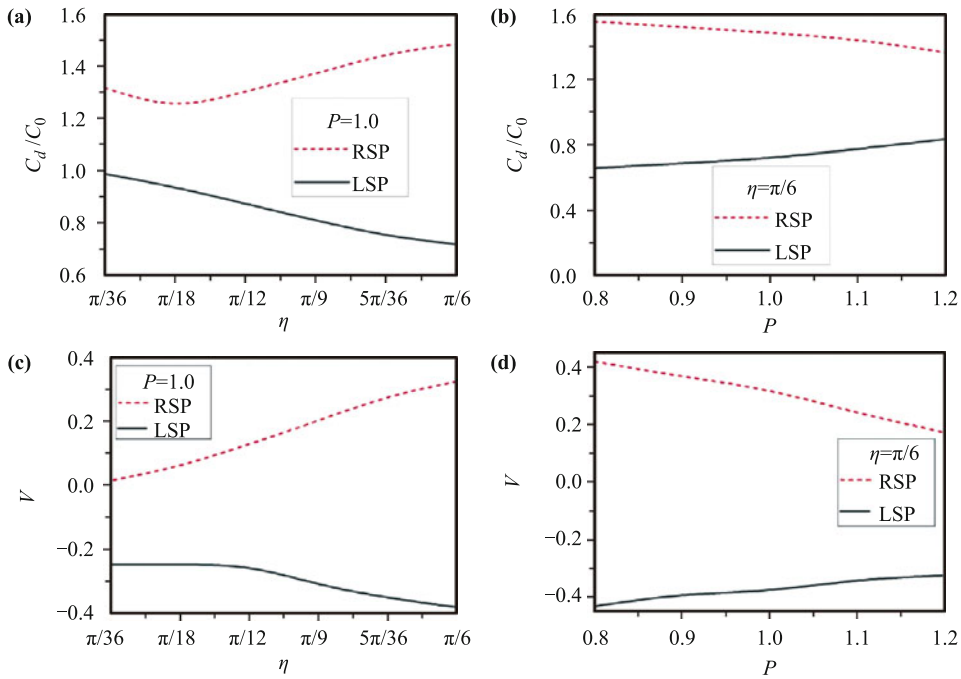

Fig. 5 LSP (left scattering point, *black solid curves*) and RSP (right scattering point, *red dash curves*) for the $\mathcal{C}$ and $\mathcal{V}$ defects as functions of η and P, respectively.

initial momentum of the soliton; thus, a large η means better soliton mobility, whereas a smaller power P also improves the mobility. Therefore, a traveling soliton with a larger η and smaller P will gain better transmissivity, which explains the wider domain between the LSP and RSP. Note that, in Fig. 5, the RSP and LSP curves are all monotonous against the defect parameter, except for the RSP in Fig. 5(a). The RSP in Fig. 5(a) first decreases and then begins to increase as η increases; this behavior is due to the smaller value of η, which is caused by the trapping effect of the defect on the moving soliton. This effect can also be viewed in Fig. 5(c) for the LSP (black solid curve) at $\eta \approx \pi/12$.

Figures 4(c) and (d) also show chaotic behavior of the T and R curves between the LSP and RSP under certain values of (η, P). This chaos is caused by trapping of the soliton by the defect. For the $\mathcal{C}$ defect, trapping occurs when $C_d/C_0 > 1$, which means that the coupling between the defect waveguides is stronger than the other couplings. This stronger coupling helps the defect to trap the soliton. For the $\mathcal{V}$ defect, trapping occurs when $V < 0$, which can be understood from the Schrödinger equation [cf. Eq. (1)], in which β_n acts as the effective potential. When $V < 0$, the local effective potential of the defect waveguide is smaller than that of the others, so the defect constructs a potential well for the traveling wave packet. Therefore, this defect can attract and trap the soliton. However, the coupling effect (for the $\mathcal{C}$ defect) and attractive effect (for the $\mathcal{V}$ defect) cannot be too strong, for Figs. 4(c) and (d) show that either too deep a defect potential or too strong an attractive effect will cause complete scattering (RSP for the $\mathcal{C}$ defect and LSP for the $\mathcal{V}$ defect) of the soliton. To identify the stable trapping areas against the environmental parameters (i.e., η and P) for both types of defects, we plot the trapping area in the (C_d, η) and (C_d, P) planes in Fig. 6 and in the (V, η) and (V, P) planes in Fig. 7. As explained above, solitons with a larger P and a smaller η have weaker mobility; therefore, these types of soliton are more easily trapped by the defect, so the area increases for larger P and smaller η.

4 Conclusion

The objective of this work is to study the interaction between a traveling soliton and two types of defects. These defects, which we call the $\mathcal{C}$ point defect and $\mathcal{V}$ point defect, are constructed by varying the local waveguide propagation parameter in the center of waveguide arrays, respectively. Transmission, reflection, scattering, and trapping of the traveling soliton in both types of defects are identified under different environmental parameter settings, including the total power of the soliton P, the initial kick applied to the soliton η, and the strength of each type of defect, which is labeled C_d for the $\mathcal{C}$ defect and V for the $\mathcal{V}$ defect. The solitons can be transmitted across the defect when the defect is weak. When the

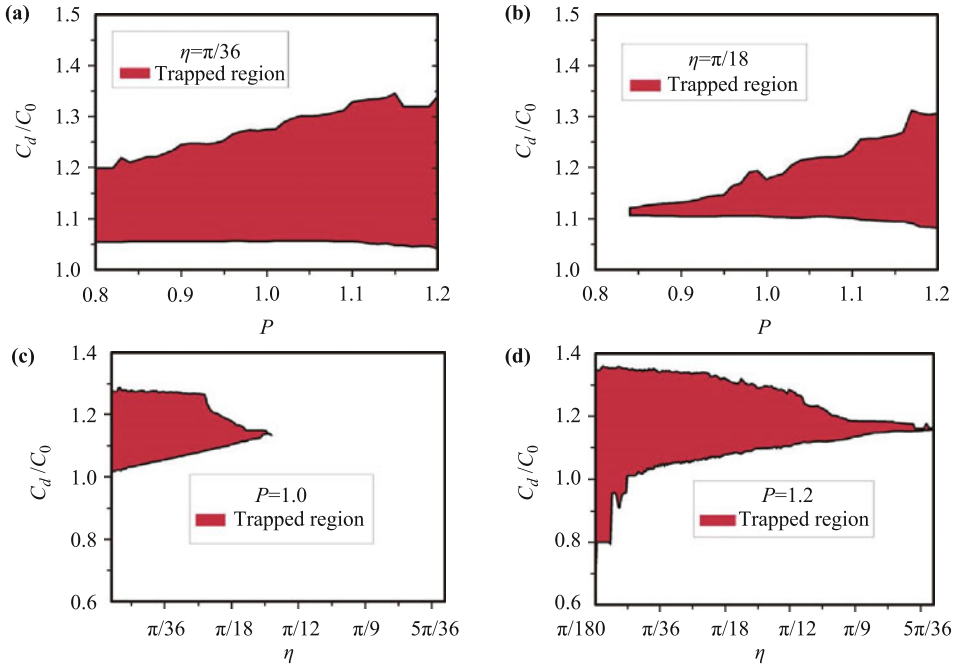

Fig. 6 Red color areas are the trapping areas. **(a,b)** The areas vs. P with different value of η ($\eta = \pi/36$ and $\pi/18$, respectively). **(c,d)** The areas vs. η with different value of P ($P = 1.0$ and 1.2, respectively).

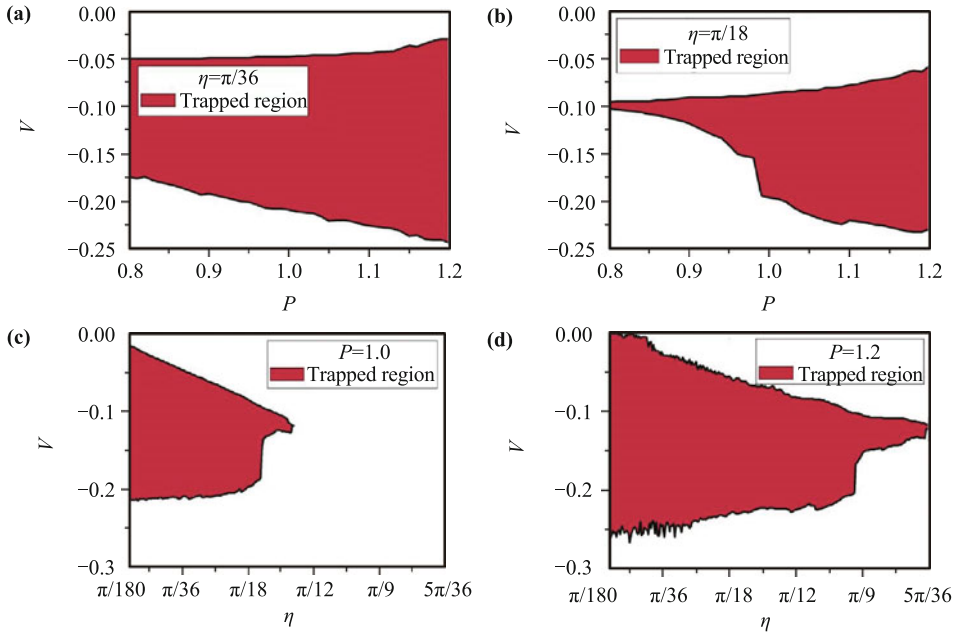

Fig. 7 Red color areas are the trapping areas. **(a,b)** The areas vs. P with different value of η ($\eta = \pi/36$ and $\pi/18$, respectively). **(c,d)** The areas vs. η with different value of P ($P = 1.0$ and 1.2, respectively).

defect becomes stronger, the soliton is destroyed by its scattering effect. At the same time, under certain parameters, the soliton may be trapped by the defect. The conditions leading to trapping are clearly identified. If the strength of the defect continues to increase, the soliton will ultimately be totally reflected by the defect. Note that the results of this work are not limited to nonlinear optics but can be expanded to other subjects concerning the dynamics of soliton motion, such as a matter-wave soliton in the context of Bose–Einstein condensates trapped in a deep optical lattice, e.g. [26–29].

Acknowledgements This work was supported by the National Natural Science Foundation of China (Grant Nos. 11104083, 11204089, and 61172011).

References

1. F. Lederer, G. I. Stegemanb, D. N. Christodoulides, G. Assanto, M. Segev, and Y. Silberberg, Discrete solitons in optics, *Phys. Rep.* 463(1–3), 1 (2008)
2. D. N. Christodoulides, F. Lederer, and Y. Silberberg, Discretizing light behaviour in linear and nonlinear waveguide lattices, *Nature* 424(6950), 817 (2003)
3. I. L. Garanovich, S. Longhi, A. A. Sukhorukova, and Y. S. Kivshar, Light propagation and localization in modulated photonic lattices and waveguides, *Phys. Rep.* 518(1–2), 1 (2012)
4. Z. Chen, M. Segev, and D. N. Christodoulides, Optical spatial solitons: Historical overview and recent advances, *Rep. Prog. Phys.* 75(8), 086401 (2012)
5. C. Lou, L. Tang, D. Song, X. Wang, J. Xu, and Z. Chen, Novel spatial solitons in light-induced photonic bandgap structures, *Front. Phys.* 3(1), 1 (2008)
6. D. N. Christodoulides and E. D. Eugenieva, Blocking and routing discrete solitons in two-dimensional networks of nonlinear waveguide arrays., *Phys. Rev. Lett.* 87(23), 233901 (2001)
7. V. Ahufinger, A. Sanpera, P. Pedri, L. Santos, and M. Lewenstein, Creation and mobility of discrete solitons in Bose-Einstein condensates, *Phys. Rev. A* 69(5), 053604 (2004)
8. R. A. Vicencio and M. Johansson, Discrete soliton mobility in two-dimensional waveguide arrays with saturable nonlinearity, *Phys. Rev. E* 73(4), 046602 (2006)
9. Y. V. Kartashov, V. A. Vysloukh, and L. Torner, Soliton shape and mobility control in optical lattices, *Progress in Optics* 52, 63 (2009)
10. Y. S. Kivshar and B. A. Malomed, Dynamics of solitons in nearly integrable systems, *Rev. Mod. Phys.* 61(4), 763 (1989)
11. V. V. Konotop, O. A. Chubykalo, and L. Vázquez, Dynamics and interaction of solitons on an integrable inhomogeneous lattice, *Phys. Rev. E* 48(1), 563 (1993)
12. D. Cai, A. R. Bishop, N. Grønbech-Jensen, and B. A. Malomed, Moving solitons in the damped Ablowitz-Ladik model driven by a standing wave, *Phys. Rev. E* 50(2), R694 (1994)
13. U. Peschel, R. Morandotti, J. S. Aitchison, H. S. Eisenberg, and Y. Silberberg, Nonlinearly induced escape from a defect state in waveguide arrays, *Appl. Phys. Lett.* 75(10), 1348 (1999)

14. R. Morandotti, H. S. Eisenberg, D. Mandelik, Y. Silberberg, D. Modotto, M. Sorel, C. R. Stanley, and J. S. Aitchison, Interactions of discrete solitons with structural defects, *Opt. Lett.* 28(10), 834 (2003)
15. L. Morales-Molina and R. A. Vicencio, Trapping of discrete solitons by defects in nonlinear waveguide arrays, *Opt. Lett.* 31(7), 966 (2006)
16. M. I. Molina, I. L. Garanovich, A. A. Sukhorukov, and Y. S. Kivshar, Discrete surface solitons in semiinfinite binary waveguide arrays, *Opt. Lett.* 33(15), 2332 (2006)
17. M. I. Molina and Y. S. Kivshar, Nonlinear localized modes at phase-slip defects in waveguide arrays, *Opt. Lett.* 33(9), 917 (2008)
18. Y. Li, W. Pang, Y. Chen, Z. Yu, J. Zhou, and H. Zhang, Defect-mediated discrete solitons in optically induced photorefractive lattices, *Phys. Rev. A* 80(4), 043824 (2009)
19. X. Zhang, J. Chai, J. Huang, Z. Chen, Y. Li, and B. A. Malomed, Discrete solitons and scatttering of lattice waves in guiding arrays with a nonlinear PT-symmetricdefect, *Opt. Exp.* 22(11), 13927 (2014)
20. X. Zhang, J. Chai, D. Ou, and Y. Li, Antisymmetry breaking of discrete dipole gap solitons induced by a phase-slip defect, *Mod. Phys. Lett. B* 28(12), 1450097 (2014)
21. S. V. Dmitriev, S. V. Suchkov, A. A. Sukhorukov, and Y. S. Kivshar, Scattering of linear and nonlinear waves in a waveguide array with a PT-symmetric defect, *Phys. Rev. A* 84(1), 013833 (2011)
22. S. V. Suchkov, A. A. Sukhorukov, S. V. Dmitriev, and Y. S. Kivshar, Scattering of the discrete solitons on the PT-symmetric defects, *Eur. Phys. Lett.* 100(5), 54003 (2012)
23. A. Regensburger, M. A. Miri, C. Bersch, J. Nager, G. Onishchukov, D. N. Christodoulides, and U. Peschel, Observation of defect states in PT-symmetric optical lattices, *Phys. Rev. Lett.* 110(22), 223902 (2013)
24. M. L. Chiofalo, S. Succi, and M. P. Tosi, Ground state of trapped interacting Bose-Einstein condensates by an explicit imaginary-time algorithm, *Phys. Rev. E* 62(5), 7438 (2000)
25. J. Yang, Newton-conjugate gradient methods for solitary wave computations, *J. Comput. Phys.* 228(18), 7007 (2009)
26. O. Morsch and M. Oberthaler, Dynamics of Bose-Einstein condensates in optical lattices, *Rev. Mod. Phys.* 78(1), 179 (2006)
27. Y. Li, J. Liu, W. Pang, and B. A. Malomed, Lattice solitons with quadrupolar intersite interactions, *Phys. Rev. A* 88(6), 063635 (2013)
28. S. W. Song, L. Wen, C. F. Liu, S. C. Gou, and W. M. Liu, Ground states, solitons and spin textures in spin-1 Bose-Einstein condensates, *Front. Phys.* 8(3), 302 (2013)
29. C. Lee, J. Huang, H. Deng, H. Dai, and J. Xu, Nonlinear quantum interferometry with Bose condensed atoms, *Front. Phys.* 7(1), 109 (2012)